Extending the Electrochemical Stability Window of $Ti_3C_2T_z$ MXenes via Ta–Hf Co-Substitution for Durable Proton Exchange Membrane Fuel Cell Catalyst Supports

Haridas Parse[1], Danielle Sviri Belilty[1], Bar Favelukis[1], Mathias Krämer[2], Andrea M. Mingers[2], Sukanta Chakrabartty[1], Noam Eliaz[1], Baptiste Gault[2, 3], Dierk Raabe[2], Maxim Sokol[1] and Brian Rosen[1]*

1. Department of Material Science and Engineering, Tel Aviv University, Ramat Aviv, 69987001, Israel
2. Max Planck Institute for Sustainable Materials, Düsseldorf 40237, Germany
3. Present address: Univ Rouen Normandie, CNRS, INSA Rouen Normandie, Groupe de Physique des Matériaux, UMR 6634, F-76000 Rouen, France

* Corresponding Author: barosen@tauex.tau.ac.il

Supplementary information

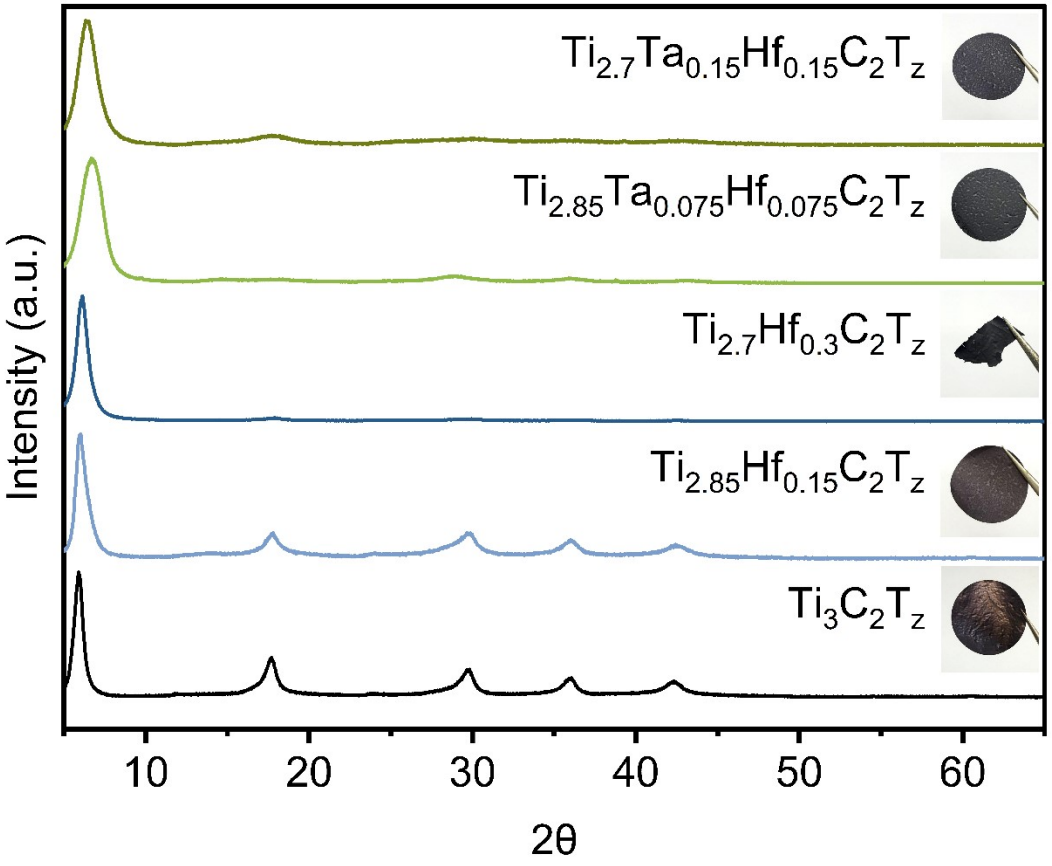

Figure S1. Comparative XRD pattern of the pristine $Ti_3C_2T_z$, $Ti_{2.85}Hf_{0.15}C_2T_z$, $Ti_{2.7}Hf_{0.3}C_2T_z$, $Ti_{2.85}Ta_{0.075}Hf_{0.075}C_2T_z$ and $Ti_{2.7}Ta_{0.15}Hf_{0.15}C_2T_z$. Insert shows freestanding films of as synthesized MXenes.

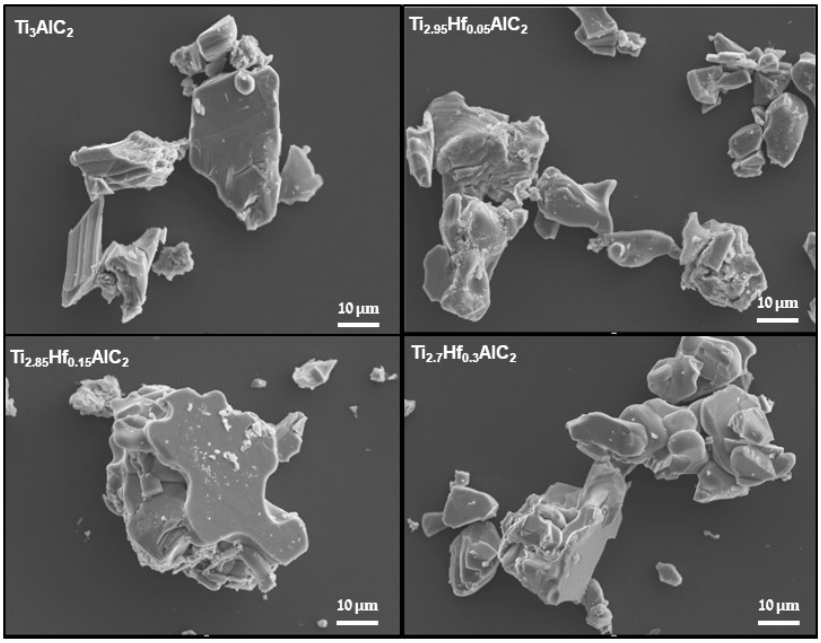

Figure S2. SEM images of the pristine Ti_3AlC_2, $Ti_{2.95}Hf_{0.05}AlC_2$, $Ti_{2.85}Hf_{0.15}AlC_2$ and $Ti_{2.7}Hf_{0.3}AlC_2$.

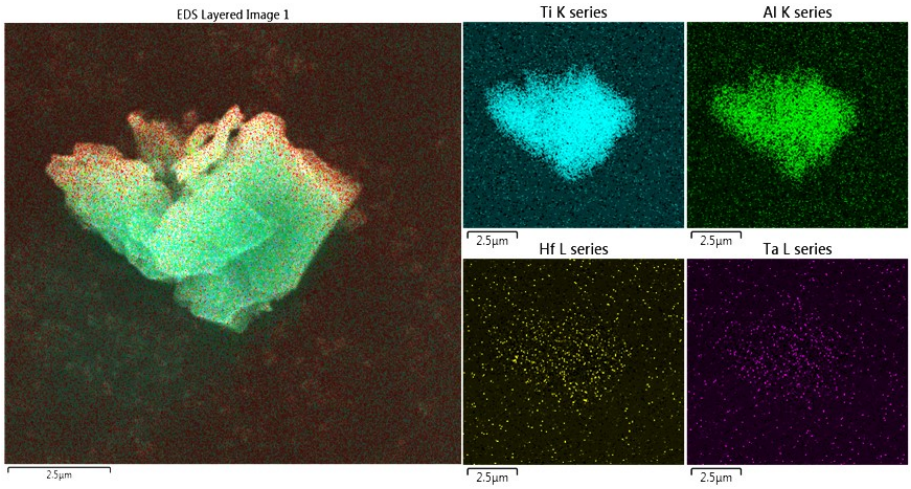

Figure S3. SEM-EDS elemental mapping of the $Ti_{2.85}Ta_{0.075}Hf_{0.075}AlC_2$.

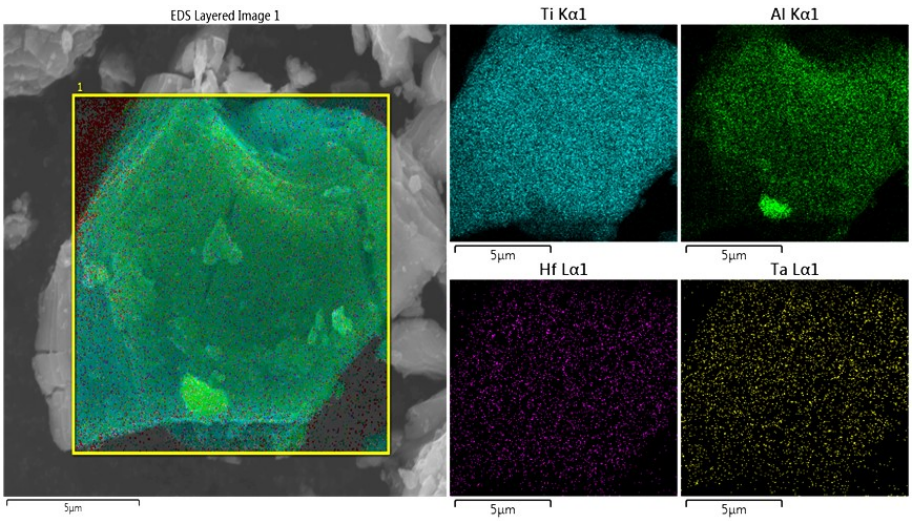

Figure S4. SEM-EDS elemental mapping of the $Ti_{2.7}Ta_{0.15}Hf_{0.15}AlC_2$.

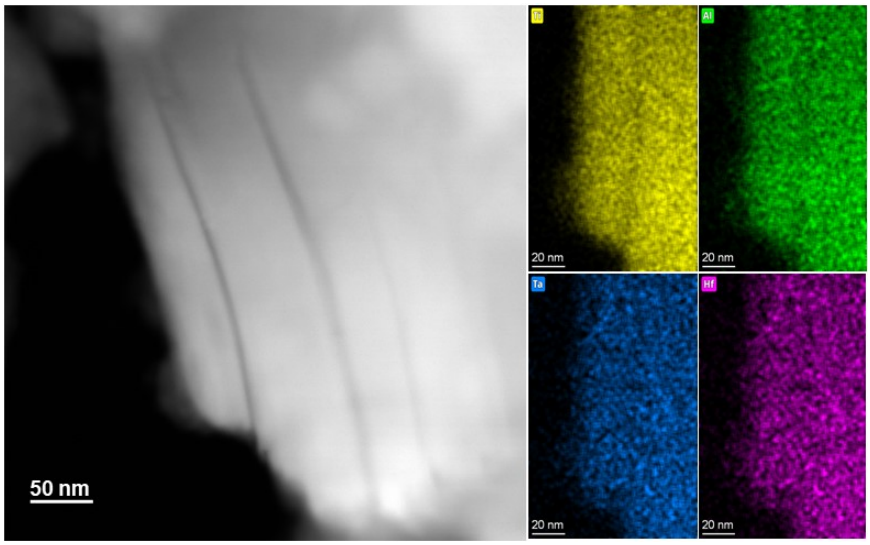

Figure S5. TEM-EDS elemental mapping of the $Ti_{2.7}Ta_{0.15}Hf_{0.15}AlC_2$.

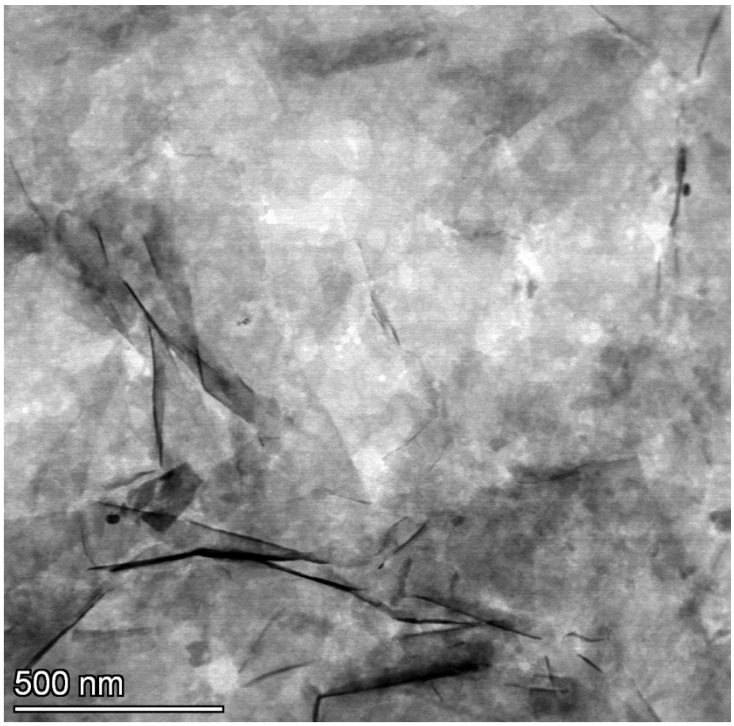

Figure S6. HR-TEM image of $Ti_{2.7}Ta_{0.15}Hf_{0.15}C_2T_z$ after scanning to the 0.9 V vs. RHE at 0.167 mV/s scan rate in the 0.5 M H_2SO_4 showing localized oxidation.

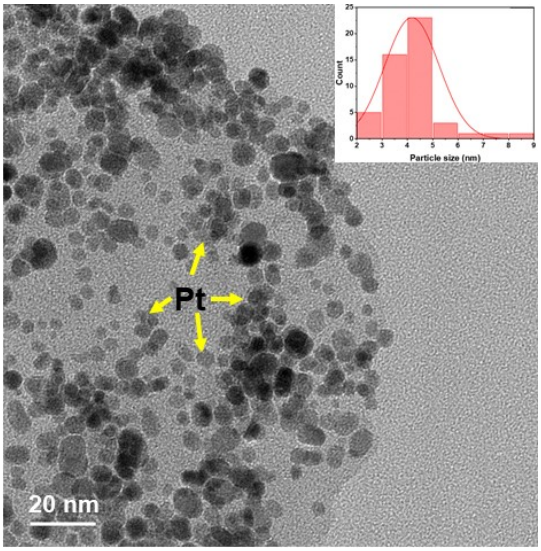

Figure S7. Bright field TEM images of the Pt loaded $Ti_{2.7}Ta_{0.15}Hf_{0.15}C_2T_z$. Inset indicate the average particle distribution of the Pt.

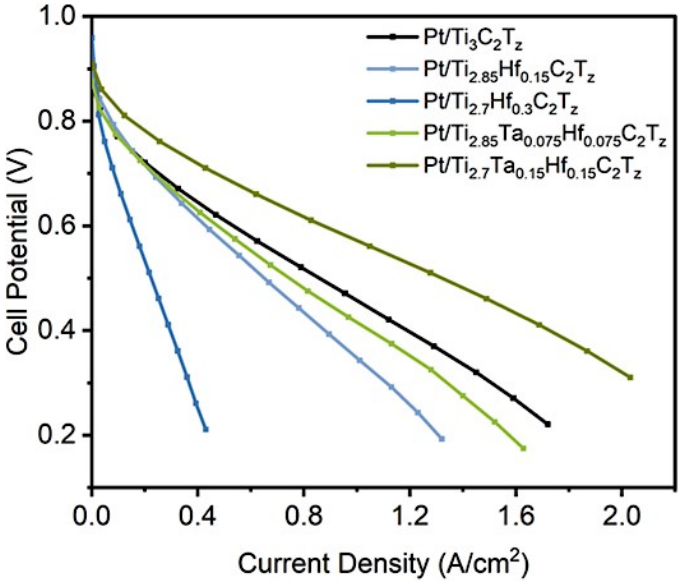

Figure S8. Comparative polarization curve using commercial Pt/C cathode and the Pt anode supported by $Pt/Ti_3C_2T_z$, $Pt/Ti_{2.85}Hf_{0.15}C_2T_z$, $Pt/Ti_{2.7}Hf_{0.3}C_2T_z$ $Pt/Ti_{2.85}Ta_{0.075}Hf_{0.075}C_2T_z$ and $Pt/Ti_{2.7}Ta_{0.15}Hf_{0.15}C_2T_z$.

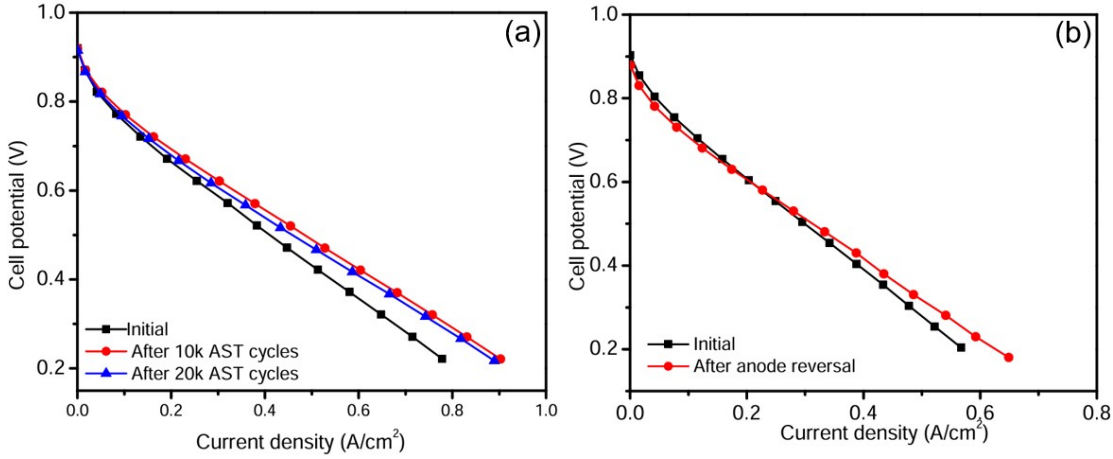

Figure S9. Comparative AST polarization curves of fuel cell cycled between 0.6 to 0.9 V using state-of-the-art Pt/C cathode and Pt anode supported by (a) $Ti_{2.7}Ta_{0.075}Hf_{0.075}C_2T_z$. (b) Polarization curves for 5 cm^2 fuel cell using Pt/C cathode and Pt supported by $Ti_{2.7}Ta_{0.075}Hf_{0.075}C_2T_z$ before and after anode reversal measurement.

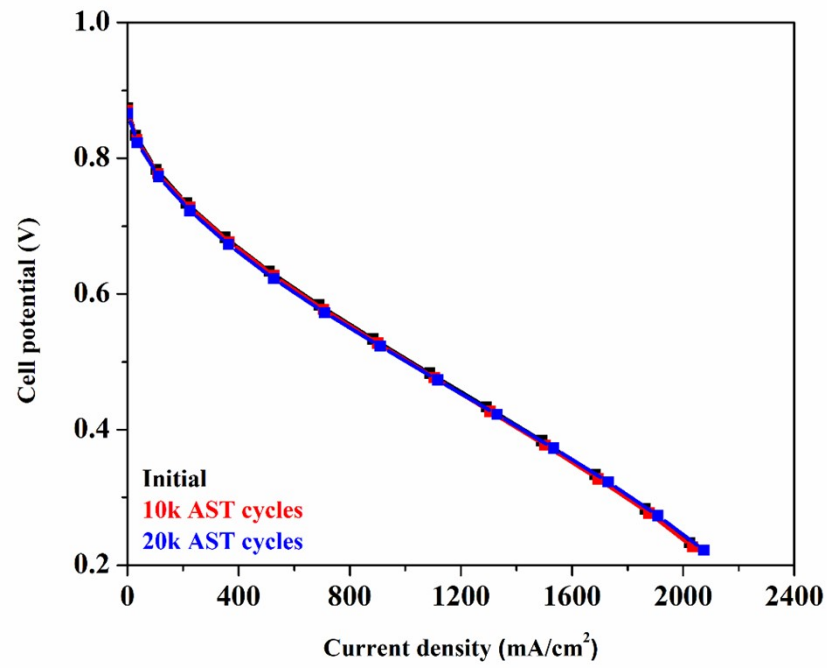

Figure S10. AST curves for a 5 cm^2 PEM fuel cell cycled between 0.6-0.8 V using commercial Pt/C cathode and a Pt anode supported by $(Ti_{0.95}Ta_{0.05})_3C_2T_z$. b) Polarization curves for a 5 cm^2 PEM fuel cell with a Pt/C cathode and a Pt anode supported by $(Ti_{0.95}Ta_{0.05})_3C_2T_z$ before and after anode reversal. Adv Funct Materials, Volume: 34, Issue: 10, First published: 03 November 2023, DOI: (10.1002/adfm.202309749).

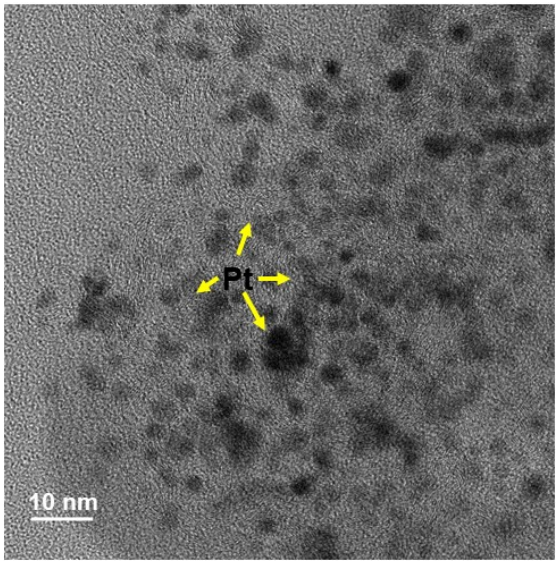

Figure S11. Bright-field TEM image of Pt/$Ti_{2.7}Ta_{0.15}Hf_{0.15}C_2T_z$ recovered from the PEMFC anode catalyst layer after 20k AST cycles between 0.6-0.9V.